

# Phenolic foams, modified by nano-metallic oxides, improved in mechanical strengths and friability

Yuxiang Zhu<sup>1</sup> · Zhengzhou Wang<sup>1,2</sup>

Received: 27 January 2016 / Accepted: 7 June 2016 / Published online: 4 July 2016  
© Iran Polymer and Petrochemical Institute 2016

**Abstract** Two kinds of nano-metallic oxides (nano- $\text{Al}_2\text{O}_3$  and nano- $\text{ZrO}_2$ ) were introduced separately into phenolic (PF) foams, and a series of PF foams modified with different loadings of the two nano-oxides were prepared. The test results of mechanical properties indicated that the flexural, compressive and impact strengths of the PF foams, modified by nano- $\text{Al}_2\text{O}_3$  at 5 phr loading, increased by 33, 46 and 51 % in the above order, and the strengths of the PF foams modified by nano- $\text{ZrO}_2$  at 5 phr loading increased by 31, 30 and 49 % in the same order, compared to the corresponding data of pure PF foam. The pulverization ratio of the modified PF foams decreased gradually with the increase in nano-oxides contents. The pulverization ratio of the PF foam modified by nano-oxides at 5 phr, decreased to 2.3 % for  $\text{Al}_2\text{O}_3$  and that of  $\text{ZrO}_2$  decreased to 2.2 %, which were quite lower than the pure PF foam value of 8 %. The combustion characteristics of the PF foams, modified by the nano-oxides, were evaluated by the limiting oxygen index (LOI), UL-94 and cone calorimetry tests. The LOI values of the foams modified by both nano- $\text{Al}_2\text{O}_3$  and nano- $\text{ZrO}_2$  decreased slightly with an increase in the loading of the nano-oxides, still all above 36 %. The UL 94 test results indicated that all foams could pass a V0 rating. The cone calorimeter results showed that the peak heat release rates of the modified foams were lower than 50 kW/m<sup>2</sup>.

Moreover, thermal stability of the foams modified by the nano-oxides was investigated.

**Keywords** Phenolic foams · Nano-metallic oxides · Mechanical strengths · Friability

## Introduction

Phenolic (PF) foams have recently attracted much attention due to their excellent flame-retardant properties compared with polyurethane (PU) foams and polystyrene (PS) foams in the field of building insulation materials [1]. However, PF foams have some serious shortcomings such as brittleness and pulverization, which greatly limit their applications in some cases [2]. Thus, researchers have focused their attention on the toughening and strengthening of PF foams [3]. The commonly used toughening agents for PF foams include polyethylene glycol (PEG), polyurethane, epoxy resins, etc. Gao et al. [4] investigated the effect of PEG on the mechanical and flame-retardant properties of phenolic foams and observed a great increase in compressive and impact strengths, but a decrease in the limiting oxygen index (LOI). Auad et al. [5] applied epoxy resins to modify PF foams and found that the modification improved the compressive, shear, and friable properties of the PF foam; nonetheless, the flammability of the modified foam increased greatly. Moreover, polyurethane prepolymer has often been used to toughen PF foams [6].

During the last two decades, nanomaterials have been used to toughen and strengthen polymeric materials [7, 8]. The introduction of small amounts of nanomaterials into the polymer matrix can combine the advantages of the polymer matrix and the discrete nanomaterials and result in great improvements on thermal and mechanical properties [9]. Several researchers have also employed many kinds of

✉ Zhengzhou Wang  
zwang@tongji.edu.cn

<sup>1</sup> School of Materials Science and Engineering, Tongji University, Shanghai 201804, People's Republic of China

<sup>2</sup> Key Laboratory of Advanced Civil Engineering Materials, Tongji University, Ministry of Education, Shanghai 201804, People's Republic of China

nanomaterials with different morphologies as additives to modify phenolic resin and its foams. For example, Ma et al. [10] used elastic nanoparticles of nitrile butadiene rubber (NBR) to toughen phenolic resin and found that the impact and flexural strengths of the toughened resin were significantly improved due to the chemical reaction occurring between the matrix and the nano-oxides. Yu et al. [11] studied the preparation of nano carboxylic acrylonitrile butadiene rubber latex tough end phenolic resins (XNBRL-PF) through in situ polymerization and found that the impact strength of XNBRL-PF was remarkably improved compared with that of pure PF. Attapulgate (ATP) and hexadecyltrimethylammonium bromide attapulgate (HTAB-ATP) nanocomposites which belong to fibrous materials were used to strengthen PF foams, and it was found that the compressive strength, thermal stability and pulverization were improved [12]. Yang et al. [13] observed that the mechanical properties and thermal stability of the PF foams modified by multi-walled carbon nanotubes were all improved. Carbon nanoparticles would promote the compressive strength, thermal stability and thermal conductivity of the foams; typically, the foam structure became more uniform and regular at the same time [14]. It has also been reported that nano-metallic oxides such as nano- $\text{Al}_2\text{O}_3$  and nano- $\text{ZrO}_2$  have good effect on the mechanical properties of polymer materials [15–17]. Especially,  $\text{ZrO}_2$  has been used as a toughening component and presents a good toughening effect [18]. However, to our knowledge, there are no publications on the use of two nano-oxides to modify PF foams.

In this paper, attempts have been made to prepare PF foams with improved mechanical strengths and friability while maintaining their excellent flame-retardant properties by means of two nano-oxides, i.e., nano- $\text{Al}_2\text{O}_3$  and nano- $\text{ZrO}_2$ . The mechanical properties and pulverization ratio of the PF foams modified by the two nano-oxides were investigated. Moreover, the flame-retardant properties of the modified foams were evaluated by the LOI, UL 94 and cone calorimetry tests.

## Experimental

### Materials

Phosphorus acid, *p*-toluene sulfonic acid, *n*-pentane and Tween-80 were purchased from Sinopharm Chemical Reagent Co. (Shanghai, China) and used without further purification. Nano- $\text{Al}_2\text{O}_3$  and nano- $\text{ZrO}_2$  aqueous dispersions were supplied by Suzhou Yougao Nano Materials Co., Ltd (both with solid content of 40 wt % and the average particle sizes (D50) of 162 nm for nano- $\text{Al}_2\text{O}_3$  and 191 nm for nano- $\text{ZrO}_2$ . Resol-type phenolic resin was provided by Shandong Shengquan Chemical Co., Ltd. (Shandong, China).

**Table 1** Formulations of phenolic foams

Sample code	Phenolic resin (phr)	Nano- $\text{Al}_2\text{O}_3$ (phr)	Nano- $\text{ZrO}_2$ (phr)
PF	100	0	0
PFA11	100	1	0
PFA12	100	2	0
PFA13	100	3	0
PFA15	100	5	0
PFA16	100	6	0
PFZr1	100	0	1
PFZr2	100	0	2
PFZr3	100	0	3
PFZr5	100	0	5
PFZr6	100	0	6

Surfactant, 5 phr; curing agent, 9 phr; blowing agent, 6 phr

### Preparation of modified phenolic foams

The resol-type phenolic resin, Tween-80 (surfactant), and nano-aluminum aqueous dispersion or nano-zirconium aqueous dispersion were added into a mixer at room temperature. The mixture was stirred vigorously and treated ultrasonically. The curing agent (phosphoric acid: *p*-toluene sulfonic acid: water = 1:2:2, mass ratio) and *n*-pentane (foaming agent) were then added to the above mixture while stirring vigorously and quickly. The obtained viscous mixture was poured into the mold and cured at 80 °C for 1 h. To maintain the density of the foam ( $16 \pm 0.5 \text{ kg/m}^3$ ) constant, the same amount of the mixture was introduced into the mold. The obtained foam was carefully cut as test samples. The formulations of phenolic foams are presented in Table 1.

### Measurements and characterization

#### Optical microscope

The microstructure of pure and modified phenolic resin foams were observed by an XPL-30TF transreflective polarizing microscope (Shanghai Weituo Instrument Co., Shanghai, China) on transmission types.

#### LOI and UL-94 vertical burning test

Limiting oxygen index was measured by an HC-2 oxygen index meter (Jiangning Analysis Instrument Co.) according to GB/T2406-2009. The specimens used for the test were  $80 \times 10 \times 10 \text{ mm}^3$ . UL-94 vertical burning test was carried out on a CFZ-2-type horizontal and vertical burning tester (Jiangning Analysis Instrument Co., Nanjing, China) according to the UL-94 test standard. The dimensions of the specimens used were  $130 \times 13 \times 3 \text{ mm}^3$ . Five samples

were used in each experiment, and the result of LOI was an average value.

### Thermogravimetric analysis

Thermogravimetric analysis (TGA) was examined using an STD Q600 (simultaneous differential scanning calorimetry—TGA) thermo-analyzer instrument (TA Co., New Castle, DE, USA) at a heating rate of 10 °C/min under a nitrogen atmosphere. The weight of all samples was kept within 5 mg in an Al<sub>2</sub>O<sub>3</sub> pan and heated from room temperature to 800 °C.

### Cone calorimeter test

Cone calorimeter test (CCT) was carried out on an FTT cone calorimeter following the procedure according to ISO 5660. The dimension of samples was 100 × 100 × 20 mm<sup>3</sup>. All the specimens were exposed horizontally to an external heat flux of 35 kW/m<sup>2</sup>. Various combustion properties such as time to ignition (TTI), heat release rate (HRR), average heat release rate (AHRR) and peak heat release rate (PHRR) were measured. Two samples were used in each test, and the average results were given.

### Scanning electron microscope (SEM)

The microstructure of the residue of the burned foams after the CCT test was observed by the Hitachi S-2360N SEM.

### Pulverization ratios

The pulverization ratio was obtained by the following method. The size of each foam was 50 × 50 × 50 mm<sup>3</sup>. A weight of 200 g was put onto the sample which was placed on a 300 mesh abrasive paper. The samples were pushed back and forth with a constant force 30 times on the paper. Each single-pass friction distance was 250 mm. The pulverization ratio was measured by the weight loss of a sample after friction, which was calculated according to Eq. (1):

$$\text{Pulverization ratio} = \frac{M_1 - M_2}{M_1} \times 100\%, \quad (1)$$

where  $M_1$  is the weight before friction and  $M_2$  the weight after friction.

### Mechanical properties

The flexural strength of foams was tested by a CMT5105 universal testing machine, according to GB/T20974-2014 (specified GB/T8812.1-2007), and the dimension of the samples was 120 × 25 × 20 mm<sup>3</sup>. The compressive strength of the foam was measured by a DXLL-5000

universal testing machine according to GB/T 20974-2014 (specified GB/T8813-2008) and its dimension was 50 × 50 × 50 mm<sup>3</sup>. The impact strength of each sample was tested according to GB/T1043.1-2008 and its dimension was 80 × 10 × 4 mm<sup>3</sup>. At least five samples were tested to obtain an average value for the mechanical tests.

## Results and discussion

### Mechanical properties

The testing results of flexural and compressive strengths of pure PF foam and PF foams modified by nano-Al<sub>2</sub>O<sub>3</sub> and nano-ZrO<sub>2</sub> are given in Figs. 1 and 2, respectively. It can

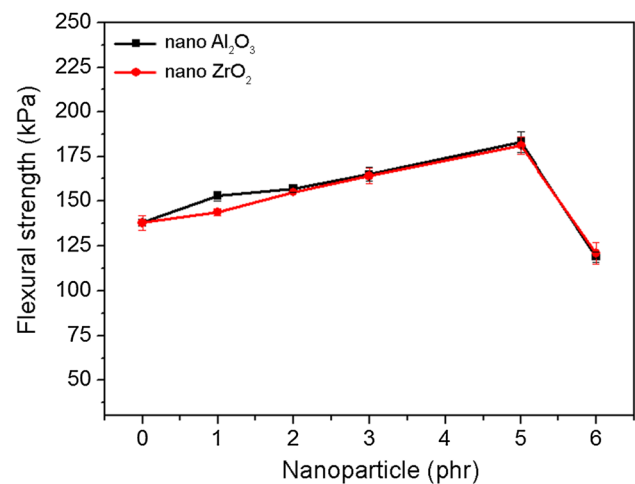


**Fig. 1** Flexural strength of pure PF and PF foams modified with different loadings of nano-oxides

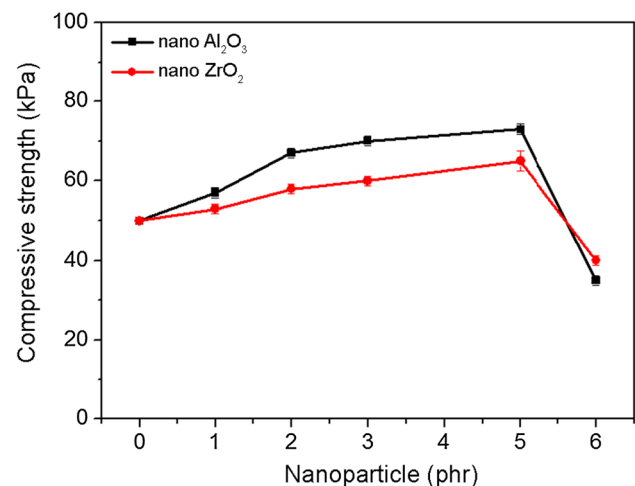


**Fig. 2** Compressive strength of pure PF and PF foams modified with different loadings of nano-oxides

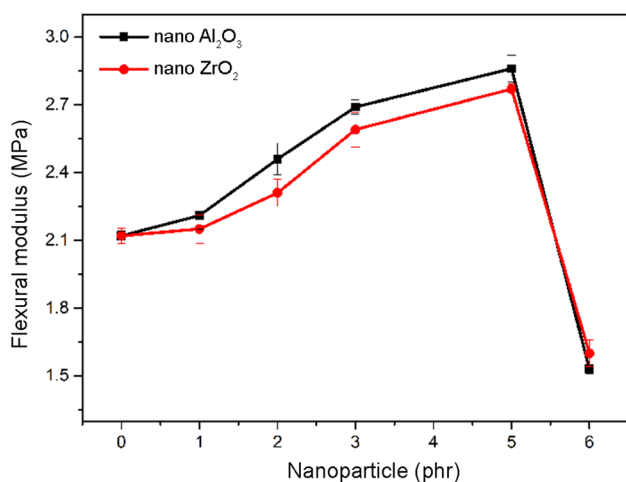


**Fig. 3** Flexural modulus of pure PF and PF foams modified with different loadings of nano-oxides

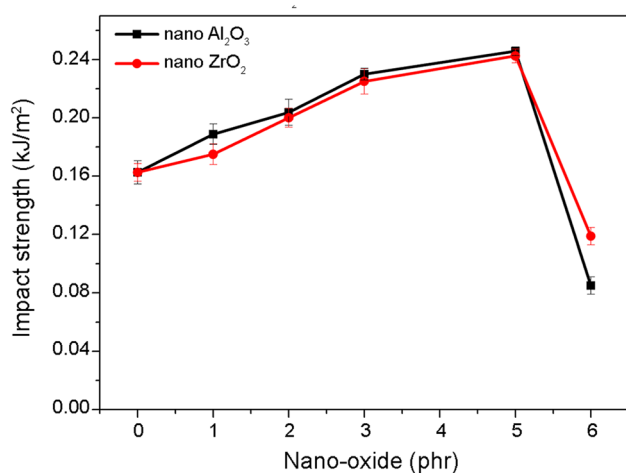


**Fig. 4** Impact strengths of pure PF and PF foams modified with different loadings of nano-oxides

be seen from Fig. 1 that the flexural strengths of both nano-Al<sub>2</sub>O<sub>3</sub> and nano-ZrO<sub>2</sub> modified PF foams first increase with an increase in the loading, then reach a maximum value at 5 phr and finally decrease sharply after 5 phr loading. Compared to pure PF foam, the flexural strengths of nano-Al<sub>2</sub>O<sub>3</sub> and nano-ZrO<sub>2</sub> modified PF foams at 5 phr loading increase by 33 % and by 31 %, respectively. The flexural moduli of PF foams are shown in Fig. 3. It is evident in Fig. 3 that the moduli exhibit similar variation trends as the strengths. As can be seen from Fig. 2, the influence of nano-Al<sub>2</sub>O<sub>3</sub> or nano-ZrO<sub>2</sub> on the compressive strength of PF foam is quite similar to that of each nano-oxide on the flexural strength. The compressive strengths of the PF foams modified by nano-Al<sub>2</sub>O<sub>3</sub> and nano-ZrO<sub>2</sub> are about 46 and 30 %, respectively, higher than that of pure PF foam.

Figure 4 shows the impact strengths of pure PF foam and the modified PF foams. As shown in Fig. 4, the impact strength also increases first with the addition of nanoparticles, then reaches a maximum value at 5 phr and decreases greatly after that loading. The increase in the mechanical properties caused by the incorporation of the nano-oxides into the PF foam is probably because these rigid nano-oxides can promote the nucleation process of the foam, and thus make the cells uniform and strong [19]. When the foam with the nano-oxides receives force, stress concentration is generated on the oxides, which can trigger crazing absorbing energy and hinder the development of cracks. It thus results in increases in the strengths and moduli [20]. Nano-Al<sub>2</sub>O<sub>3</sub> is more effective in improving the mechanical strengths of PF foam than nano-ZrO<sub>2</sub>. However, too much nano-oxides tend to cause agglomeration which can trigger cracks directly and lead to destruction of the foam [21]. As shown in Figs. 1, 2 and 4, the strengths of the modified foams at 6 phr of the nano-oxides decrease sharply. The reason for this great drop can be attributed to the larger cell size and the non-uniform cell structure, which are adverse to the ability to undergo high external force for the modified PF foams.

#### Pulverization ratios

Friability is always a deadly drawback of PF foams and so great efforts have been done to improve it [11, 22]. Figure 5 presents the pulverization ratio of pure PF foam and PF foams modified with nano-oxides. The pulverization ratio of pure PF foam is 8.16 %. As shown in Fig. 5, the pulverization ratio of the modified PF foams decreases gradually with the increase in the content of the nano-oxides. The pulverization ratio of the modified PF

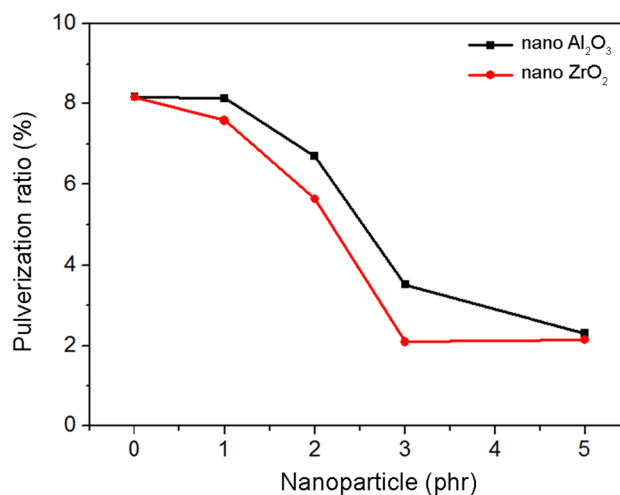


**Fig. 5** Pulverization ratios of PF and PF foams modified with different loadings of nano-oxides

foams are all lower than that of pure PF foam. Specially, the ratios of the PF foams modified with nano- $\text{Al}_2\text{O}_3$  and nano- $\text{ZrO}_2$  at 5 phr decrease to 2.3 and 2.2 % in the given order. It is obvious that the pulverization ratio of the modified foams with nano- $\text{ZrO}_2$  is lower than that of the modified foams with nano- $\text{Al}_2\text{O}_3$  at the same loading level, indicating that nano- $\text{ZrO}_2$  is more effective in reducing the friability of PF foam than nano- $\text{Al}_2\text{O}_3$ , because  $\text{ZrO}_2$  has not only a strengthening effect but also some toughening effect on the matrix [18].  $\text{ZrO}_2$  has been used as toughening agent for  $\text{Al}_2\text{O}_3$  ceramics; this indicates that  $\text{ZrO}_2$  has better toughness than  $\text{Al}_2\text{O}_3$  [23, 24]. The reason for the decrease in the pulverization can be explained by the fact that the existence of the nano-oxides in cell ribs and cell walls of the modified foams can undergo external force and thus improve the damage endurance in the foams.

## Microstructures

Optical microscope was used to study the effect of the nano-oxides on the microstructure of PF foams. As shown in Fig. 6, all the foams consist of a majority of closed cells. We used the software, Image J, to calculate the cell sizes of the foams, and the methods of the detailed analysis are provided in the publication [25]. It is found that the average diameter of the cells in the modified foams first decreases slightly and then increases with the addition of nano-oxides compared to those of pure PF foam. The average diameter of cells in the modified foams of pure PF foam is 168  $\mu\text{m}$ , while the values of PFA11, PFA13, PFA15 and PFA16 are 165, 161, 164 and 251  $\mu\text{m}$ , respectively, and those of PFZr1, PFZr3, PFZr5 and PFZr6 are 167, 152, 136 and 246  $\mu\text{m}$ , respectively. Moreover, the shapes of the cells modified by the nano-oxides change obviously with increasing the loading

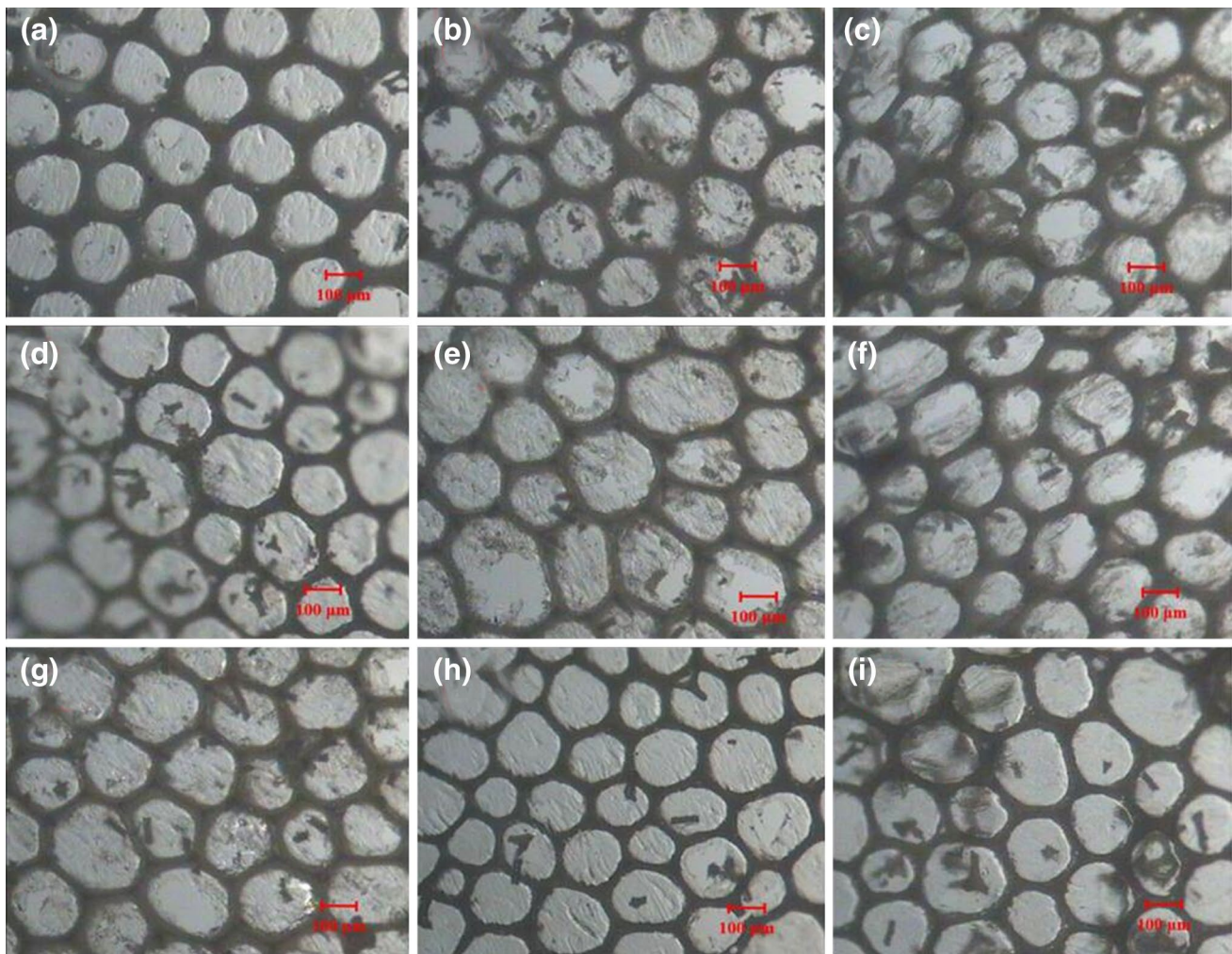


**Fig. 6** Optical images of **a** PF, **b** PFA11, **c** PFA13, **d** PFA15, **e** PFA16, **f** PFZr1, **g** PFZr3, **h** PFZr5 and **i** PFZr6. The magnification of all images is  $\times 40$

of nano-oxides, especially at high loadings. The reason for the above change is because the nano-oxides in the foams would initiate more micro-bubbles, increase the number of cells and decrease the combination of the cells. It is known that the thickness of the cell membrane decreases as the number of cells increases [19, 26]. However, due to easy aggregation of the nano-oxides at a higher loading (6.0 phr), the cell size becomes larger and the cell structure becomes non-uniform, as shown in Fig. 6e, i.

**Combustion behavior**

The flame-resistant behavior of pure PF foam and the modified foams by the nano-oxides was evaluated by the LOI and UL-94 vertical burning test. As shown in Fig. 7, the LOI values of the foams modified by nano-Al<sub>2</sub>O<sub>3</sub> change a little below 3 phr, while the values of the foams modified by nano-ZrO<sub>2</sub> decrease slightly. When the loading of the nano-oxides increases to 5 phr, the LOI values decrease further. This may be due to the nucleation effect of the nano-oxides, which will make the cell membrane a little thinner and easier to burn [24]. Meanwhile, the nano-oxides are nonflammable and will not greatly affect the flame-retardant properties of phenolic foams. The LOI values of the modified foams are above 36 %, and all the foams can pass the UL-94 V0 rating, as shown in Fig. 7, which indicates the foams still maintain excellent flame-retardant properties.

The combustion characteristics of the modified PF foams were also studied using the cone calorimeter. The heat release rate (HRR) curves of the modified PF foams are shown in Figs. 8 and 9, and the corresponding data are listed in Table 2. The peak heat release rate (PHRR) of

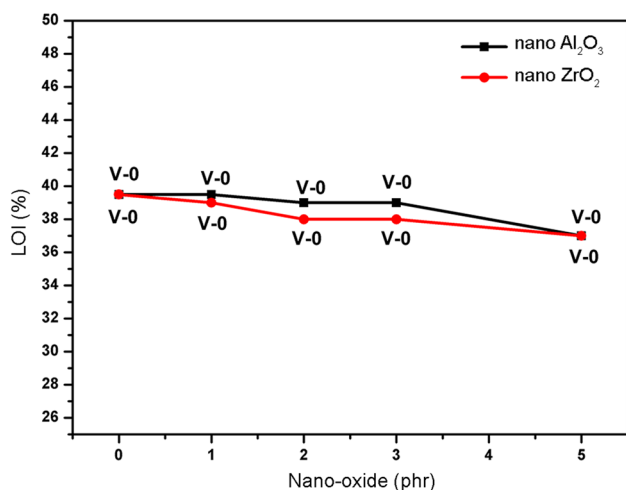


Fig. 7 Effect of nano-oxides on the LOI of phenolic foams

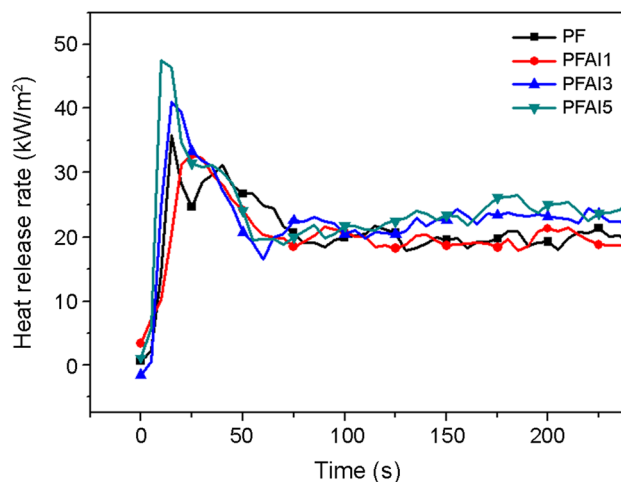


Fig. 8 Heat release rate curves of the modified foams with different loadings of nano-Al<sub>2</sub>O<sub>3</sub> (35 kW/m<sup>2</sup>)

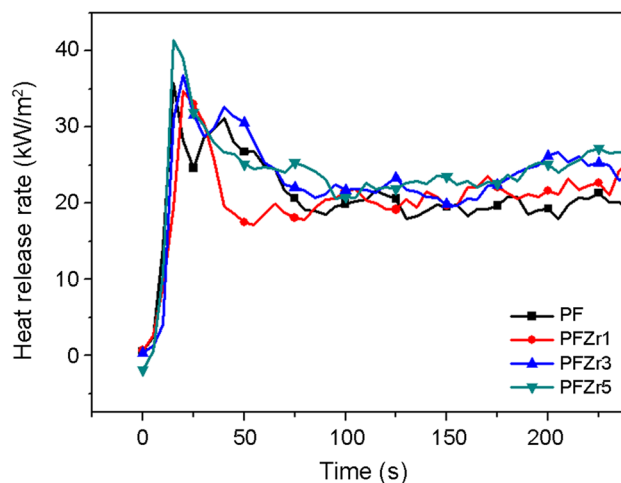


Fig. 9 Heat release rate curves of the modified foams with different loadings of nano-ZrO<sub>2</sub> (35 kW/m<sup>2</sup>)

Table 2 Cone calorimetry data of nano-oxides modified foams

Sample code	Time to ignition	PHRR <sup>a</sup> (kW/m <sup>2</sup> )	THR <sup>b</sup> (MJ/m <sup>2</sup> )
Pure	4	36	5.0
PFA11	8	33	4.9
PFA13	5	41	5.5
PFA15	2	48	5.8
PFZr1	10	35	4.8
PFZr3	6	37	5.6
PFZr5	7	41	5.7

<sup>a</sup> Peak heat release rate

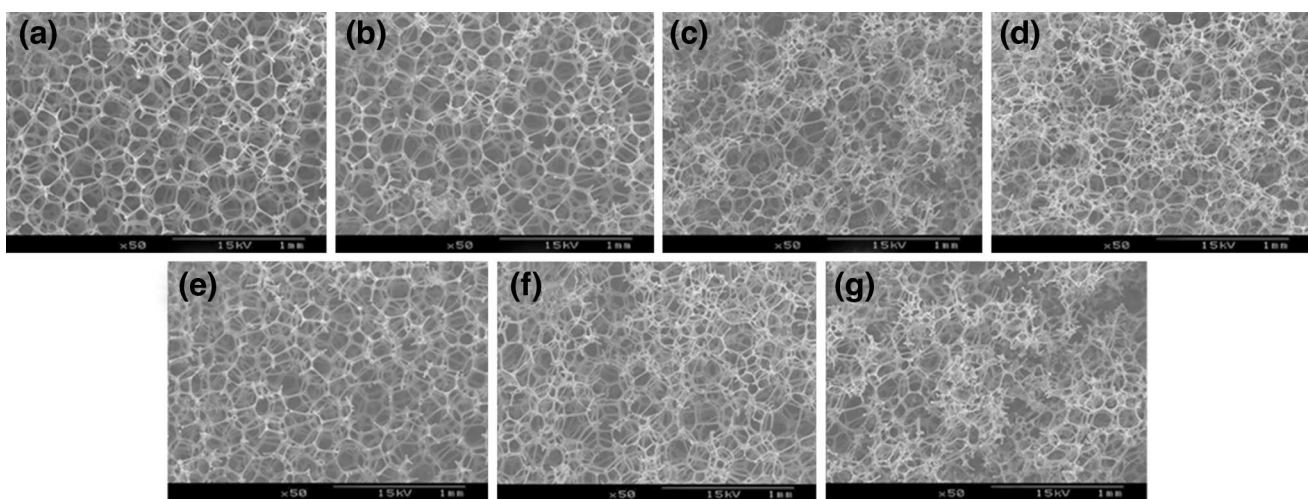
<sup>b</sup> Total heat release

pure PF foam is  $36 \text{ kW/m}^2$ , and the PHRR value decreases to  $33 \text{ kW/m}^2$  (sample PFA11) and to  $35 \text{ kW/m}^2$  (sample PFZr1) at low loading of the nano-oxides (1 phr). A further increase in the loading of the nano-oxides leads to a slight increase in the PHRR value, but all the values are below  $50 \text{ kW/m}^2$ . The effects of the nano-oxides on the average heat release rate (AHRR) and total heat release (THR) results are similar to their effects on PHRR. The above results may be explained by the fact that the weak nucleation effect of the nano-oxides at low loading (1 phr) brings about a slight change on the cell membrane of the foams, and the non-combustible oxides may lead to a decrease in the PHRR. The slight decrease in PHRR of the PF foam with 1 phr loading can be explained by the reason that as the non-combustible nanoparticles are incorporated into the PF foams, the dispersed inflammable nanoparticles hinder the decomposition of the polymer chains of PF foams. However, a further increase in the nano-oxides will make the cell membrane of the foams thinner, which would be easier to burn. As seen from SEM images of the char residue after cone calorimeter test (Fig. 10), the cell structure of the char left by the modified foams with higher loadings of the nano-oxides becomes less regular (even damaged in some parts) compared to that of the pure PF foam and the modified foams with low loadings of the nano-oxides.

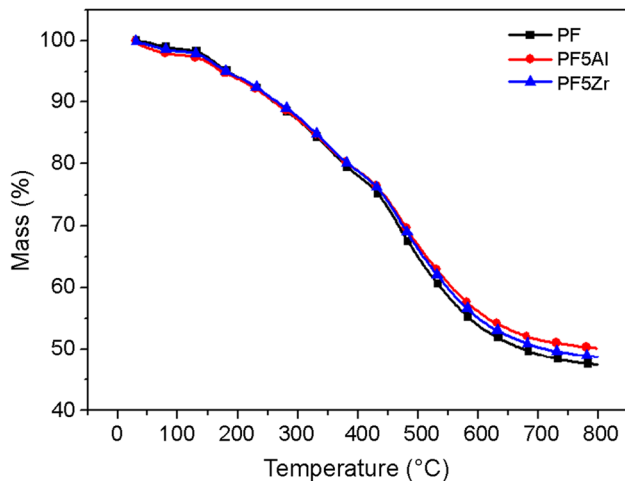
### Thermal decomposition

Figure 11 shows the TGA curves of the pure PF foam and PF foams modified by the two nano-oxides. It can be seen from the derivative thermogravimetric (DTG)

curves (Fig. 12) that pure PF foam has five decomposition steps. The initial decomposition below  $100 \text{ }^\circ\text{C}$  is mainly due to the evaporation of residual water and blowing agent (*n*-pentane, boiling point  $36.1 \text{ }^\circ\text{C}$ ); the second decomposition step occurring at about  $160 \text{ }^\circ\text{C}$  may be on account of the dehydration of further curing of PF foams [6]; the third step at around  $250 \text{ }^\circ\text{C}$  and the fourth step at nearly  $350 \text{ }^\circ\text{C}$  may belong to the decomposition and evaporation of surfactant (Tween-80) and some curing agents (phosphorus acid and boron acid). The fifth step (the main decomposition step) is located in the range of  $400\text{--}800 \text{ }^\circ\text{C}$ , which is attributed to the decomposition of phenolic resin [27]. The thermal decomposition of the modified PF foams is also in five steps, quite similar to the one of pure PF foam. The incorporation of the two nano-oxides seems to have less influence on the first to fourth decomposition steps and only affects the fifth step. The  $T_{\text{max}}$  (the temperature at a maximum weight loss) values of the modified foams, sample PFA15 and sample PFZr5 at the fifth step, are  $470$  and  $471 \text{ }^\circ\text{C}$ , respectively, which are slightly higher than that of pure PF foam ( $465 \text{ }^\circ\text{C}$ ). The reason for the increase of  $T_{\text{max}}$  values of the modified foams may be because the nanoparticles can protect the PF resin from thermal degradation by restricting the polymer chains in the PF foams [21]. Moreover, the weight loss of samples PFA15 and PFZr5 at a fixed temperature in the range of  $400\text{--}800 \text{ }^\circ\text{C}$  is less than that of the pure PF foam. The improvement in the thermal stability at high temperatures is easy to understand, since highly thermally stable nano-oxides are mixed with relatively thermally unstable phenolic resin [11].



**Fig. 10** SEM images of the residues after the cone calorimetry test: **a** PF, **b** PFA11, **c** PFA13, **d** PFA15, **e** PFZr1, **f** PFZr3 and **g** PFZr5



**Fig. 11** TGA curves of PF, PFA15 and PFZr5

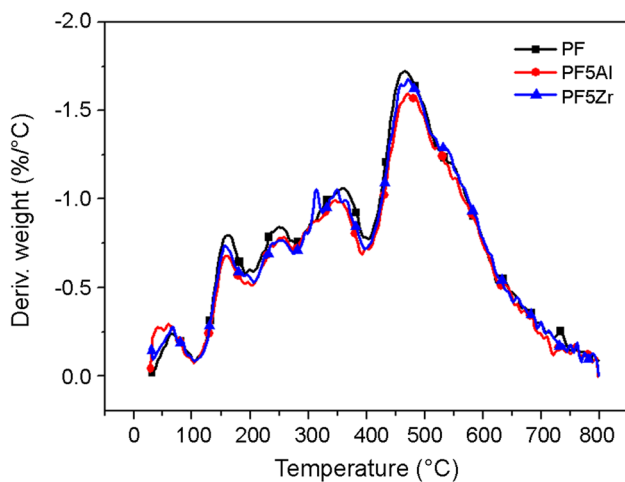


**Fig. 12** DTG curves of PF, PFA15 and PFZ

## Conclusion

Two nano-metallic oxides, i.e., nano- $\text{Al}_2\text{O}_3$  and nano- $\text{ZrO}_2$ , were used to modify phenolic (PF) foams. It was found that the incorporation of suitable amounts of the nano-oxides into the PF foams leads to a great increase in the flexural, compressive and impact strengths. Moreover, the pulverization ratio of the PF foams was reduced due to the addition of nano-oxides, where nano- $\text{ZrO}_2$  was more effective in reducing the pulverization ratio than nano- $\text{Al}_2\text{O}_3$ . The LOI values of the modified foams were all above 37 %, and their UL-94 ratings were V0. The cone calorimeter results proved that the peak heat release rates of the modified foams were below  $50 \text{ kW/m}^2$ . The TGA results indicated that the residues of the foams modified with the nano-oxides left at high temperatures increased compared to that of pure PF foam.

**Acknowledgments** This work was financially supported by the National Natural Science Foundation of China (Nos. U1205114 and 21174106).

## References

1. Lei S, Guo Q, Shi J, Liu L (2010) Preparation of phenolic-based carbon foam with controllable pore structure and high compressive strength. *Carbon* 48:2644–2646
2. Huang Y, Wang C, Huang Y, Guo G, Nutt SR (2010) Enhancing specific strength and stiffness of phenolic microsphere syntactic foams through carbon fiber reinforcement. *Polym Compos* 31:256–262
3. Gietl TD, Lengsfeld HD, Altstädt VD (2006) The efficiency of various toughening agents in novel phenolic type thermoset resin systems. *J Mater Sci* 41:8226–8243
4. Hu XM, Wang DM, Cheng WM, Zhou G (2014) Effect of polyethylene glycol on the mechanical property, microstructure, thermal stability, and flame resistance of phenol–urea–formaldehyde foams. *J Mater Sci* 49:1556–1565
5. Auad ML, Zhao L, Shen H, Nutt SR, Sorathia U (2007) Flammability properties and mechanical performance of epoxy modified phenolic foams. *J Appl Polym Sci* 104:1399–1407
6. Yang H, Wang X, Yu B, Yuan H, Song L, Hu Y, Yuen RK, Yeoh GH (2013) A novel polyurethane prepolymer as toughening agent preparation, characterization, and its influence on mechanical and flame retardant properties of phenolic foam. *J Appl Polym Sci* 128:2720–2728
7. Wang W, Zhang H, Dai Y, Hou H, Dong H (2015) Effects of various nanomaterials on the properties of starch/poly(vinyl alcohol) composite films formed by blow extrusion process. *Iran Polym J* 24:687–696
8. Rezaei Abadchi M, JalaliArani A (2015) Synergistic effects of nano-scale polybutadiene rubber powder (PBRP) and nanoclay on the structure, dynamic mechanical and thermal properties of polypropylene (PP). *Iran Polym J* 24:805–813
9. Schmid G (1992) Large clusters and colloids. *Metals in the embryonic state*. *Chem Rev* 92:1709–1727
10. Ma H, Wei G, Liu Y, Zhang X, Gao J, Huang F, Tan B, Song Z, Qiao J (2005) Effect of elastomeric nano particles on properties of phenolic resin. *Polymer* 46:10568–10573
11. Yu Z, Li J, Yang L, Yao Y, Su Z, Chen X (2012) Synthesis and properties of nano carboxylic acrylonitrile butadiene rubber latex toughened phenolic resin. *J Appl Polym Sci* 123:1079–1084
12. Zhuang Z, He B, Yang Z (2010) Preparation and characterization of phenolic foam/HTAB-ATP nanocomposites. *Plast Rubber Compos* 39:460–464
13. Yang Z, Yuan L, Gu Y, Li M, Sun Z, Zhang Z (2013) Improvement in mechanical and thermal properties of phenolic foam reinforced with multiwalled carbon nanotubes. *J Appl Polym Sci* 130:1479–1488
14. Song SA, Chung YS, Kim SS (2014) The mechanical and thermal characteristics of phenolic foams reinforced with carbon nanoparticles. *Compos Sci Technol* 103:85–93
15. Song H, Zhang Z, Men X (2006) Effect of nano- $\text{Al}_2\text{O}_3$  surface treatment on the tribological performance of phenolic composite coating. *Surf Coat Technol* 201:3767–3774
16. Song H, Zhang Z (2006) Investigation of the tribological properties of polyfluoro wax/polyurethane composite coating filled with nano-SiC or nano- $\text{ZrO}_2$ . *Mater Sci Eng, A* 426:59–65
17. Cai H, Yan F, Xue Q, Liu W (2003) Investigation of tribological properties of  $\text{Al}_2\text{O}_3$ -polyimide nanocomposites. *Polym Test* 22:875–882

18. Malek O, Lauwers B, Perez Y, De Baets P, Vleugels J (2009) Processing of ultrafine ZrO<sub>2</sub> toughened WC composites. *J Eur Ceram Soc* 29:3371–3378
19. Lee LJ, Zeng C, Cao X, Han X, Shen J, Xu G (2005) Polymer nanocomposite foams. *Compos Sci Technol* 65:2344–2363
20. Maharsia RR, Jerro HD (2007) Enhancing tensile strength and toughness in syntactic foams through nanoclay reinforcement. *Mater Sci Eng A* 454:416–422
21. Manoylov A, Bojarevics V, Pericleous K (2015) Modeling the break-up of nano-particle clusters in aluminum- and magnesium-based metal matrix nano-composites. *Metall Mater Trans A* 46:2893–2907
22. Hu L, Zhou Y, Zhang M, Liu R (2012) Characterization and properties of a lignosulfonate-based phenolic foam. *BioResources* 7:554–564
23. Rao PG, Iwasa M, Tanaka T, Kondoh I, Inoue T (2003) Preparation and mechanical properties of Al<sub>2</sub>O<sub>3</sub>-15 wt% ZrO<sub>2</sub> composites. *Scripta Mater* 48:437–441
24. Tuan WH, Chen RZ, Wang TC, Cheng CH, Kuo PS (2002) Mechanical properties of Al<sub>2</sub>O<sub>3</sub>/ZrO<sub>2</sub> composites. *J Eur Ceram Soc* 22:2827–2833
25. Guo HM, Nicolae A, Kumar V (2015) Solid-state microcellular and nanocellular polysulfone foams. *J Poly Sci Part B* 53:975–985
26. Kharbas H, Nelson P, Yuan M, Gong S, Turng L (2003) Effects of nano-fillers and process conditions on the microstructure and mechanical properties of microcellular injection molded polyamide nanocomposites. *Polym Compos* 24:655–671
27. Strečková M, Sopčák T, Medvecký L, Bureš R, Fáberová M, Batko I, Briančin J (2012) Preparation, chemical and mechanical properties of microcomposite materials based on Fe powder and phenol-formaldehyde resin. *Chem Eng J* 180:343–353